ELSEVIER

Thermochimica Acta 296 (1997) 75–85

thermochimica acta

A calorimetric study on a cylindrical type lithium secondary battery by using a twin-type heat conduction calorimeter

Y. Saito*, K. Kanari[1], K. Takano[2], T. Masuda[3]

Electrotechnical Laboratory, Tsukuba, Ibaraki, 305, Japan

Received 16 May 1996; accepted 18 December 1996

Abstract

Thermochemical properties of a lithium secondary battery are calorimetrically studied. A twin-type heat conduction calorimeter was used and its accuracy was determined by the specific heat capacity measurement of a standard material, synthetic sapphire. The inaccuracy was smaller than 1.1% in the range of 303–343 K. The thermal transitions corresponding to crystal phase transitions of the positive electrode material, $Li_{1-x}CoO_2$, between hexagonal and monoclinic symmetry were observed. An attempt was made to measure the apparent specific heat capacity of the battery and to study its dependence on the state of charge. The influences of the diffusion of lithium ions in the electrode materials and the self-discharge to the apparent specific heat capacity are discussed. © 1997 Elsevier Science B.V.

Keywords: Intercalation; Lithium secondary battery; Scanning method; Specific heat capacity; Twin-type heat conduction calorimeter

1. Introduction

In recent years, many researchers have investigated the lithium secondary batteries because of their many intrinsic advantages such as high voltage, 3–4 V, and high energy density of 2–4 times over conventional aqueous secondary batteries.

One of the key issues of lithium secondary batteries is safety. Temperature rise and its distribution in a battery during charge and discharge affect performance and reliability of the battery, and cause serious safety hazards such as ignition, especially in the case of abuse or malfunctioning operation. Thermal design of the battery systems considering various conditions is important. In order to design the battery, heat generation mechanism of the battery reaction has to be understood and thermodynamic and thermochemical properties of materials used in the battery should be determined: specific heat capacity, thermal conductivity, and so on.

Calorimetric study is one approach to investigate such issues of lithium secondary batteries. However, there are few reports on a cylindrical type battery [1] because of the difficulty of preparing a calorimeter of sufficient accuracy and sensitivity. In this study, we have used a twin-type heat conduction calorimeter having large sample holders in which a commercial lithium battery could be packed without disassem-

*Corresponding author. Fax: 00 81 298 58 5805; e-mail: e9309@etl.go.jp.

[1]E-mail: e6505@etl.go.jp.

[2]E-mail: e6629@etl.go.jp.

[3]E-mail: e6719@etl.go.jp.

PII S0040-6031(97)00083-X

bling or breaking-up the battery into each component material. Calorimetry of the battery during charge and discharge was investigated to study heat generation from battery reactions. Apparent specific heat capacity of the battery was also estimated by the scanning method, and the influence of various factors of heat generation during temperature scanning is discussed.

2. Experimental

2.1. Sample

A commercial battery [2] called lithium ion battery, US14500 (SONY Energytec Inc.), was used as a sample. It is a cylindrical type 14 mm in diameter and 50 mm in length, and weighing approximately 19 g. It consisted of positive and negative electrodes wound spirally with a separator between them. The negative electrode is made of a copper current collector with hard carbon as an active electrode material on both sides. Hard carbon means non-graphitizable carbon in heating treatment. The positive electrode consists of an aluminum current collector and $LiCoO_2$ powder mixed with carbon powder as a conductive diluent and Polytetrafluoroethylene (PTFE) as binder. The separator is made of microporous poly-olefin film and contains a mixed solvent of propylene carbonate and diethyl carbonate with $LiPF_6$ as the supporting electrolyte in its pores. All components are packed in a metal casing. The nominal battery voltage is 3.6 V as decided from an averaged value during discharge from 4.2 to 2.5 V in 5 h, and the nominal electric capacity is 500 mA h.

2.2. Apparatus

A twin-type differential heat conduction calorimeter (C80, Setaram) was used. The size of the standard sample holder of this instrument is 17 mm in diameter and 80 mm in length and large enough to insert the test battery. Since it was possible to vary the inside temperature of the calorimeter from ambient temperature to 300 K with a maximum programmable rate of 2.0 K min^{-1}, the scanning method [3] was used for specific heat capacity measurement. The lower limit of detection of the instrument was 10 μW. The heat flow between the thermopile and the sample holder was monitored as a function of time and temperature by a computer (Personal System/V Model 2405/2410, IBM) using the software obtained from Setaram. A pair of specially designed sample holders made of stainless steel was used for the measurement of the battery. The outer size of those holders was as the same as the standard one and the inner size was set to fit the test battery. The battery was packed into one of the holders and connected to a programmable DC source (Model 7651, Yokogawa Electric Corporation) for charge and discharge of the battery and to a nanovoltmeter (Model 181, Keithley Instrument, Inc.) to measure the battery voltage, through two pairs of lead wires made of copper coated by insulator. The cross-sectional areas of the wires connected to the DC source were about 1.25 mm^2 and the others were 0.5 mm^2. A brass rod was packed into the other holder as a reference. The current and the voltage of the battery were monitored by another computer (PC-9801RX, NEC).

2.3. Calorimetry of the lithium ion battery during charge and discharge

The state of charge of the sample battery was normalized at the full charged state. The battery was charged at a constant current of 50 mA until the battery voltage reached 4.30 V and then was charged at a constant voltage of 4.30 V for about 3 h. The temperature was held at 303 K during the process. This charged battery was regarded as in the full charged state for convenience. In this paper, the state of the battery was described by the quantity of electricity, Q, discharged from the full charged state. Thus Q, is 0 mA h in the full charged battery and increased with discharging the battery.

Calorimetry of the battery during charge and discharge at 50 mA was carried out by operating the instrument isothermally. The temperature of the sample holders was held at 303 K during charge and discharge. The battery was discharged from the full charged state to 2.75 V at first, and then charged to the full charged state. Heat flow and battery voltage data were recorded every 15.0 and 10.0 s, respectively.

2.4. Measurement of specific heat capacity

The specific heat capacity of the test battery was measured by the scanning method [3]. The

temperature of the sample was held constant for 4 h before and after scanning to obtain isothermal baselines. The scanning range of temperature was between 303 and 343 K to prevent evaporation of the electrolyte at approximately 350 K and above, and the scanning rate was controlled at 0.1 K min^{-1}. Readings were recorded every 10.6 s. At first, the measurement was carried out on the full charged battery. Then, it was held at 303 K for 24 h before temperature scanning was started. After the scanning, the sample was cooled down and held at 303 K again. Next, the battery was discharged at 50 mA. The discharging current was turned off intermittently at some designated states of Q. Temperature scanning was carried out in each open circuit period between intermittent discharges and then the battery was cooled down again before next discharge. The total time of each open circuit period was 48 h while the temperature scanning, cooling down and holding at 303 K were undertaken. The temperature of the sample holders was held at 303 K during each discharging period.

In order to determine the accuracy of the measured value, specific heat capacity of a standard material, synthetic sapphire (SRM-720, NIST) was measured.

3. Results

3.1. Calorimetry of the lithium ion battery

The time constant of the delay due to heat transfer between sample and thermopile of the instrument was evaluated as 341 s [4]. Since the results of calorimetry were influenced by this delay, the measurement values had to be corrected to discuss the time dependence of heat generation behaviour. Fig. 1 shows the heat flow from the battery, P, as a function of time, t, during discharge at 50 mA constant current. The data has been corrected for the influence of the delay [4], and P corresponds to instantaneous heat generated in each time directly. The current was turned off at 35032 s when the battery voltage reached 2.75 V. The electric capacity of the test battery in the range between 4.30 and 2.75 V in battery voltage at 303 K was approximately 487 mA h. The long decay of the heat flow is observed after the current has been turned off.

The sources of the heat generation during discharge of the battery and those quantification will be discussed in detail in our next paper [4]. In this study, we mention only that the main factors of heat generation are electric resistance of the materials, electrochemical polarizations at the interface between the electro-

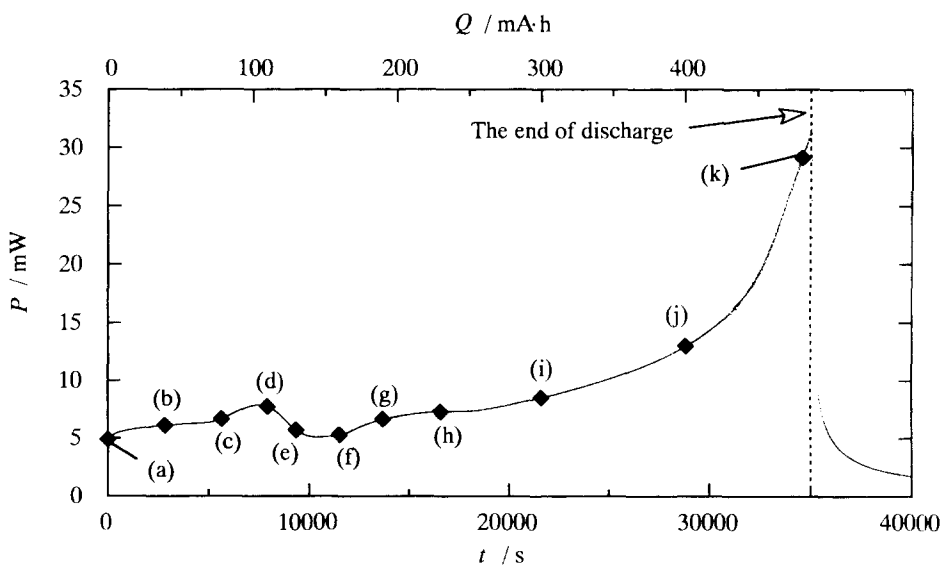

Fig. 1. Heat generation curve of a lithium ion battery during discharge at 50 mA constant current. Q means quantity of electricity discharged from full charged state of the battery. Diamonds are plotted at Q where the apparent specific heat capacity of the battery is evaluated, and they are (a) 0, (b) 40, (c) 80, (d) 110, (e) 130, (f) 160, (g) 190, (h) 230, (i) 300, (j) 400 and (k) 480 mA h.

des and the electrolyte, and electrochemical reactions. In Fig. 1, heat generation behaviour is shown in all periods of discharge with complex changes including some exothermic and endothermic peaks. The shape of the curve depends on the battery reaction, especially, the entropy change of the reaction which is decided by the composition and crystal structure of the electrode materials. The same measurement was also applied to the charging reaction [4]. In contrast to discharge, heat absorption behaviour was observed. The shape of the curve was almost identical to the discharging curve against Q axis. It means reversibility of the battery reaction.

3.2. *Temperature scanning and apparent specific heat capacity of the lithium ion battery*

The specific heat capacity of the test battery was evaluated at several states of Q pointed out with letters of alphabet in Fig. 1. Some states were selected at around 120 mA h where the curve showed interesting behaviours such as a maximum and a minimum.

Fig. 2 shows the heat flows and the battery voltages during temperature scanning for the specific heat capacity measurement. The results of a blank measurement and temperature change are shown in the last figure. Since the dummy was inserted into the sample holder of the reference side, the heat flow of the blank measurement is larger than those of sample measurements. The peaks observed at about 15 000 and 40 000 s do not correspond with heat generation or absorption because they are in the transition periods. Heat absorption peaks in scanning periods can be seen in (c), (d), (e) and (f). Especially in (d) and (e), the peaks are clearly seen, and in addition, the shapes of the heat flow curves are also different from those of the others in the initial periods of temperature scanning at about 17 000 s. These two states are located between exothermic and endothermic peaks in Fig. 1.

The battery voltage decreases monotonically during temperature scanning and shows a linearity with time and temperature except in the last two states of discharge, (j) and (k). The slope of the line, $(\Delta V/\Delta t)$, is related to the entropy change, ΔS, of the battery reaction that can be described as

$$\Delta S = nF\left(\frac{\partial V}{\partial T}\right)_P \tag{1}$$

since the scanning rate, $(\Delta T/\Delta t)$, is constant, where n and F are the number of electrons exchanged by the reaction and Faraday constant, respectively. In some figures such as (j) and (k), before or after temperature scanning, the open circuit voltage changes markedly even though it is in isothermal period.

While the isothermal baselines at 303 K before temperature scanning are not different in many of the results, they do not agree with each other after the scan. The lines are shifted upwards, and long decays are seen in states (j) and (k), though the heat loss through the lead wires were not different in all the measurements. These are caused by some heat generation this will be discussed later. When the specific heat capacity of the battery is evaluated, the baseline is important. The baseline of (h) was selected as representative and a standard because it was flat and the difference in the baseline before and after scanning was the smallest. This isothermal baseline was linearly interpolated between 303 and 343 K and the interpolated baseline was applied to all other results. The difference between heat flow curve and the interpolated baseline was calculated for both the blank and sample scannings. The difference between the value of blank and sample divided by scanning rate gave the specific heat capacity of the sample plotted in Fig. 3. These are apparent values affected by heat generation from the battery. There are peaks in states (d) and (e) due to the endothermic peaks in Fig. 2. Though there are two other small peaks at about 320 and 332 K, these are caused by the noise in the blank measurement and are not regarded as significant. On the whole, the specific heat capacity of the battery decreases gradually with discharging.

4. Discussion

4.1. *Specific heat capacity of synthetic sapphire measured by scanning method*

When the specific heat capacity is measured by the scanning method by DSC [3] a reference material, the specific heat capacity of which is accurately known, is used. The specific heat capacity of the sample is usually measured as a relative value. Instead of using a reference sample, a calibration curve can be determined using the Joule effect principle in the case of the

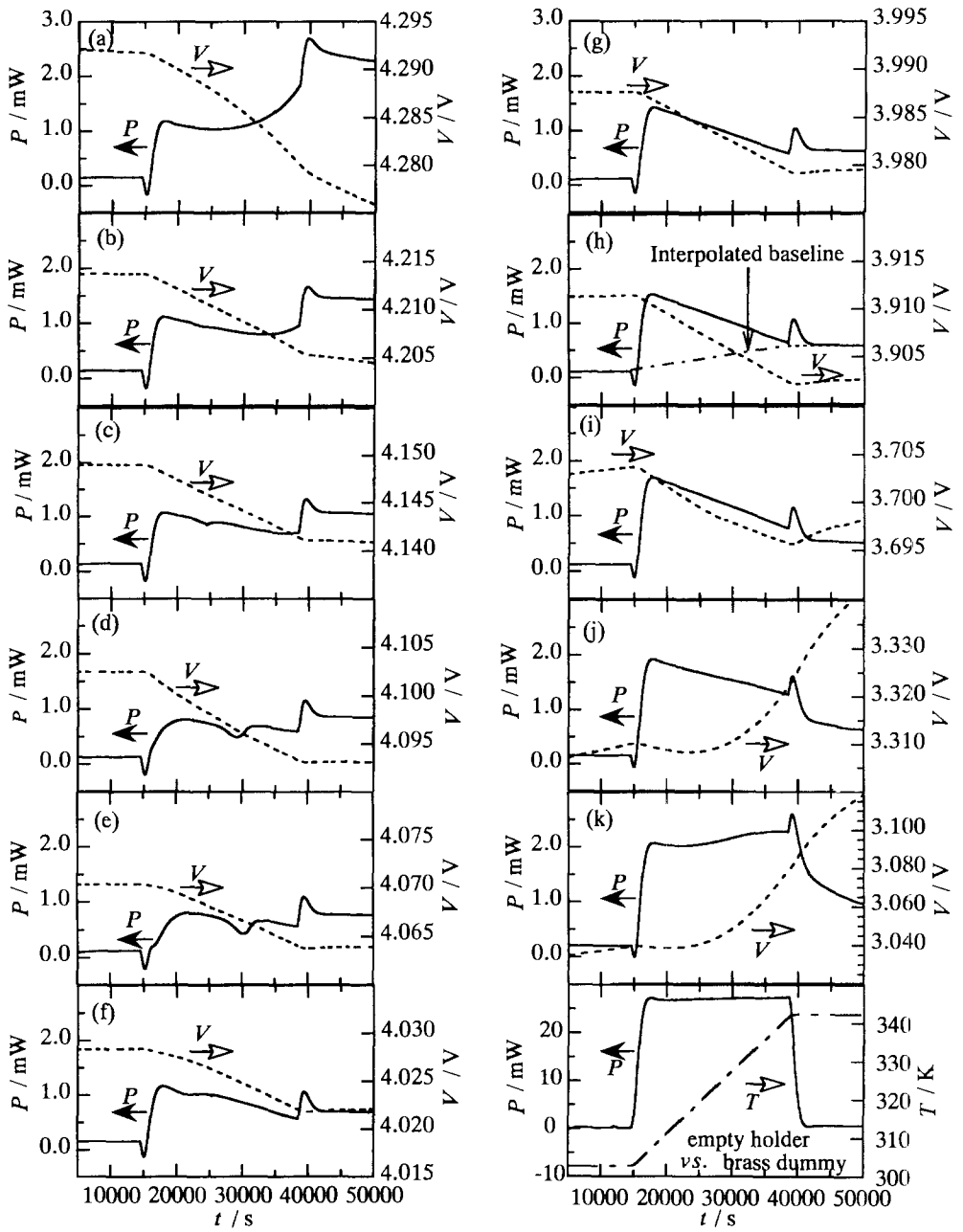

Fig. 2. Heat flow and open circuit voltage of a lithium ion battery during temperature scanning. Temperature range is from 303 to 343 K, and scan rate is 0.1 K min^{-1}. A brass rod dummy is inserted into reference side holder. The meanings of alphabet letters are as same as those of Fig. 1. The last figure shows temperature curve and heat flow of blank measurement.

twin-type calorimeter. A pair of experimental vessels including resistance heaters is put into the chambers of the calorimeter, and heat is dissipated in the sample-side holder of them. A relation between the signal detected by the thermopile and the dissipated heat is calculated and it gives the calibration coefficient at a defined temperature. Consequently, this instrument does not need any reference materials, and specific

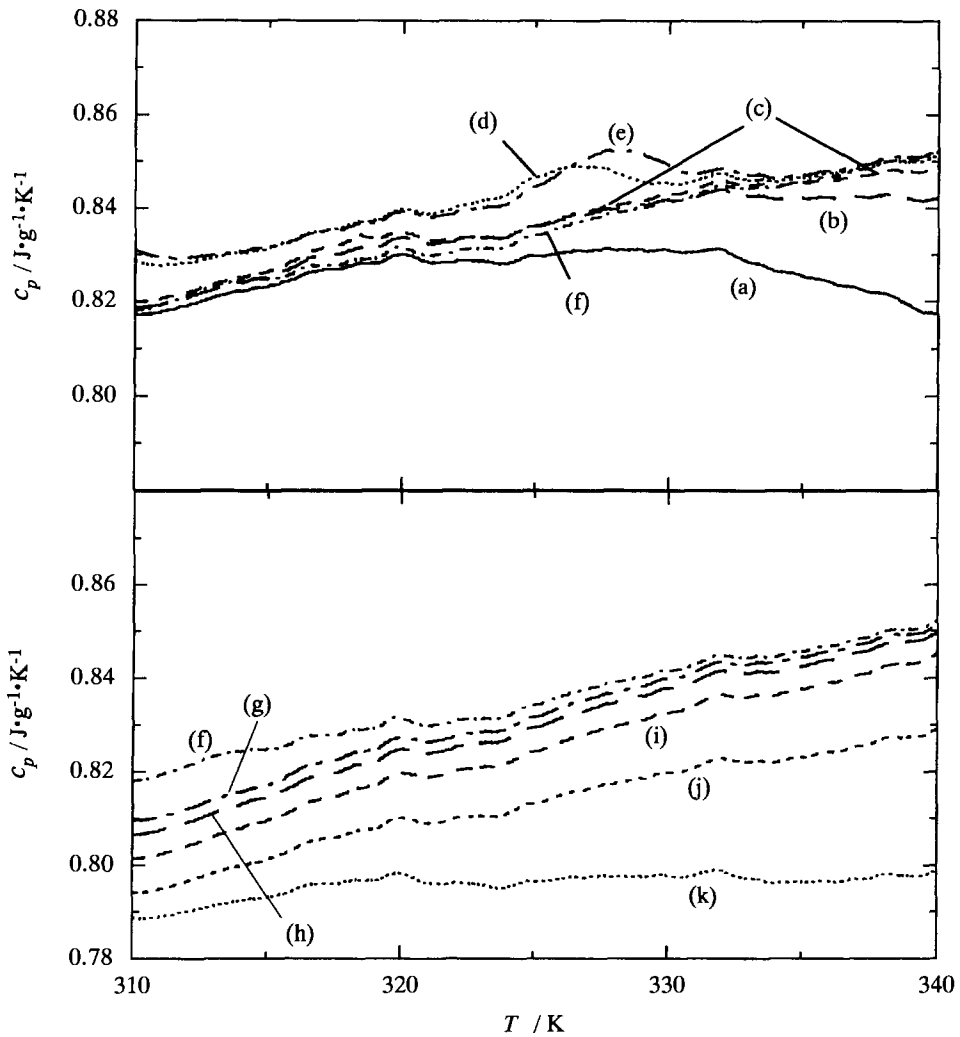

Fig. 3. Apparent specific heat capacity of a lithium ion battery at various states. The meanings of alphabet letters are as same as those of Fig. 1. An interpolated baseline of (h) in Fig. 2 is used for all states.

heat capacity of the sample is estimated readily and rapidly.

Although as small an amount of sample as possible, should be used for DSC to avoid the influence of temperature distribution in the sample, larger sample holders are used in the C80 calorimeter. In order to determine the accuracy of the specific heat capacity measurement by this instrument, experiments were carried out by using 3.8, 7.6, 15.3 and 26.0 g of sapphire. Standard vessels made of stainless steel were used as the sample holders. One of these was empty as a reference holder. The sample was packed into the other one. The holder was almost completely filled with 26.0 g of the synthetic sapphire except top part occupied by a pan while that is filled until approximately half height with 15.3 g of the sample. Fig. 4 shows the results of the specific heat capacity measurements from the synthetic sapphire. A temperature interval of 70 K between 303 and 373 K was used. A slow scan rate, 0.1 K min^{-1}, was selected to decrease the influence of the temperature distribution inside the sample holders due to the large sample size. The specific heat capacity data taken from the literature [5] are also plotted in Fig. 4. Good agreement between

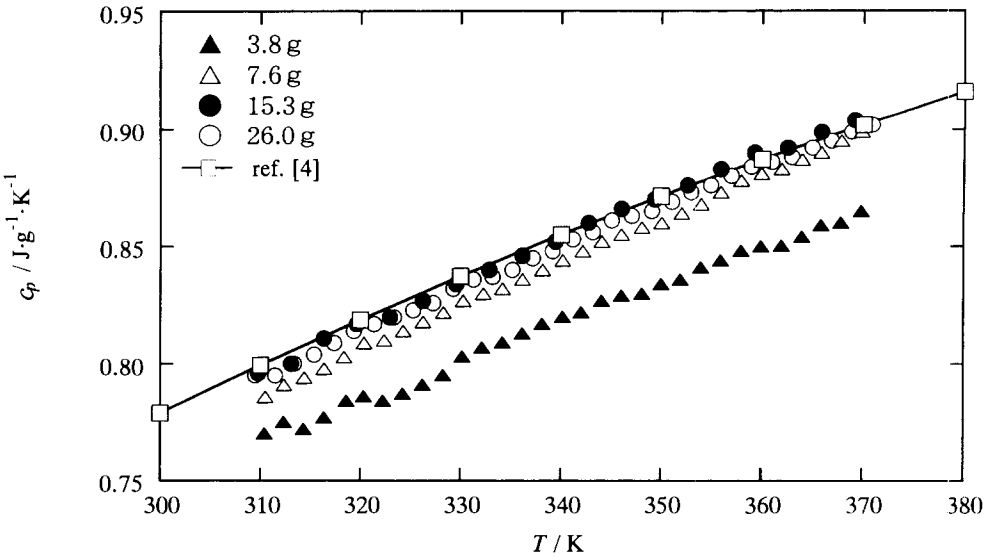

Fig. 4. Sample amount dependence of specific heat capacity measurement by a heat conduction calorimeter for synthetic sapphire. The results are compared with reference value [2].

the measured and reference values were obtained with 15.3 g and 26.0 g of the sample within an error of 0.5%, samples less than 15.3 g gave smaller values and larger errors. With this calibration, the Joule's heat is generated from almost all part of the experimental vessels uniformly. This suggests that the calibration curve cannot be applied to the experiment in which the relatively small amount of sample is packed into only lower part of the holder because of nonuniform heat transfer at the surface of the holder. The sample holder has to be packed to at least half volume with the sample in order to obtain reliable values. In the case of the lithium ion battery the size was large enough to measure its specific heat capacity.

The sample holders used for the battery were different from that used for the synthetic sapphire described above, and the inside of the holders was connected to the outside of the calorimeter through lead wires. The error in the measured values will be larger owing to heat loss through these wires, especially at high temperatures. The specific heat capacity of the synthetic sapphire was remeasured using these holders in order to estimate the error caused by the difference in the holders. As the result, the error in this system was atmost 1.1% in the range of 303–343 K.

4.2. *Crystal phase transition of the positive electrode material,* $Li_{1-x}CoO_2$

The battery reaction is described as

$$LiCoO_2 + C_y \leftrightarrow Li_{1-x}CoO_2 + Li_xC_y \quad (0 \le x \le 1) \tag{2}$$

The charging reaction is from left to right and x becomes larger on charging. Usually, the battery is not charged beyond $x = 0.5$ to prevent fading of the rechargeable capacity. Since lithium ions move between both electrodes during charge and discharge, these batteries are called lithium ion batteries, shuttlecock type batteries, or rocking-chair batteries. Thus the compositions of active electrode materials, $Li_{1-x}CoO_2$ and Li_xC_y, changes with x during charge and discharge as shown in Eq. (2), and it is expected that the thermochemical properties of the electrode materials also changes with charging and discharging.

In addition, it is reported that the negative electrode material, lithium intercalated carbon, shows stage structures such as LiC_6(first stage) and LiC_{12}(second LiC_{12}(second stage) [6], and they depend on the concentration of lithium ions inserted into carbon materials. As for the positive electrode material $Li_{1-x}CoO_2$, lattice distortion has been reported by

Reimers and Dahn [7]. They performed in situ x-ray diffraction measurement on $Li_{1-x}CoO_2$ by changing x electrochemically and discussed the crystal phase transitions of the material depending on x. This material crystallizes with the space group R_3m and the unit cell has hexagonal symmetry except in a narrow range around $x = 0.5$ where a monoclinic unit cell is observed. The width of this range depends on temperature, and it disappears at about 333 K and above. They also measured the electrode potential, V, against lithium metal electrode as a function of x, and discussed the relation between the transition and V.

In our experiment, the battery voltage, V, was also measured as a function of discharging time. Two slight peaks were observed in the derivative curves of the time by the battery voltage, dt/dV, in the high voltage range and these characteristics were very similar to Reimers' results. These occur at the same time as the exothermic and endothermic peaks observed in Fig. 1. Comparison between Reimers' and our results indicate that these behaviours correspond with the phase transitions between hexagonal and monoclinic symmetry. Heat generation is observed during the transition from hexagonal to monoclinic and heat absorption during the reverse transition. This suggests that the composition of the positive electrode material is $Li_{0.5}CoO_2$ at about 125 mA h of Q. At the end of discharge where $Q = 487$ mA h, the composition is assumed to be $Li_{0.9}CoO_2$ because of the rapid decrease of the battery voltage observed near $x = 0.9$ during discharge [7]. Thus the composition at the full charged state is $Li_{0.36}CoO_2$.

The crystal phase of the positive electrode material at states (d) or (e) in Fig. 1 is monoclinic. In Fig. 2, endothermic peaks are clearly observed from the battery at these states. The composition range of x where the monoclinic structure is observed becomes narrower with increasing temperature and disappears at about 333 K and above [6]. It is concluded that these peaks are due to the phase transition from monoclinic to hexagonal.

4.3. *Relaxation of lithium ion distribution in the electrodes*

In Fig. 1, when the current is turned off, heat flow, P does not disappear immediately and long decay is seen over several hours. This is called the 'end effect' for convenience. The end effect is not due to a delay in response of the experimental system since its corrections have been already made for this. This suggests that an exothermic behaviour occur in the battery even if current is not applied. One of the causes of the end effect is that of self-discharge including side reactions such as the decomposition of the electrolyte. Certainly, the electric capacity of the battery decreases gradually with charge and discharge cycles. However, the self-discharge of the lithium ion battery is rather small in general and the efficiency of charge and discharge was over 99% in our experiment at a constant temperature of 303 K. Thus the self-discharge is not the most important factor in the end effect and there are more important factors. i.e. diffusion of lithium ions to the electrode materials. Some researchers have measured the chemical diffusion coefficients of lithium ions, D, in the electrodes materials [8,9]. For example, D of $Li_{0.65}CoO_2$ was measured to be $5 \times 10^{-12}\ m^2\ s^{-1}$ by Thomas et al. [8], and Uchida et al. evaluated $D = 2.5 \times 10^{-12}\ m^2\ s^{-1}$ and $D = 1.6 \times 10^{-13}\ m^2\ s^{-1}$ in $Li_{0.4}C_6$ [9]. These are consistent with the diffusion of lithium ions not being fast enough to allow lithium ions to distribute uniformly with the intercalate or deintercalate processes and concentration gradients of lithium in the electrodes are generated during charge and discharge. Even if the current has been turned off, relaxation of these concentration occurs and probably caused heat generation.

The influence of the diffusion can be seen in Fig. 2 as the decay of the isothermal baselines of 343 K, especially, at states (a), (j) and (k). Since they are located either early or at the last stages of discharge in which a lot of lithium ions intercalated into either positive or negative electrode, the influence of lithium distribution is large. When the battery is charged or discharged a concentration gradient of lithium in the electrodes is generated. Even if the heat disappears after resting the battery for a long time, the distribution of the lithium ions does not become uniform completely at room temperature, and the diffusion of lithium ions is activated and restarted with temperature rising.

The changes of the open circuit voltage during the isothermal process in Fig. 2 can be also explained by diffusion of the lithium ions. The open circuit voltage probably does not depend on the averaged concentration of lithium in the whole electrode but on the local

concentration near the interface between each electrode and electrolyte. The self-discharge also seems to be one of the important causes of changes observed in states (a), (b), and (c) where the open circuit voltage is higher and decreases gradually. In the other states it increases.

4.4. Apparent specific heat capacity of the lithium ion battery

Since the apparent specific heat capacity of the battery shown in Fig. 3 has been calculated using the interpolated baseline of state (h), the influence of the diffusion of lithium ions are present in these results. Therefore somewhat lower values are seen in the first state, (a), and last states, (j) and (k).

If the diffusion of lithium ions causes heat generation, the heat decreases gradually with the relaxation of the concentration gradient. Hence temperature scanning from 273 to 343 K was carried out three times continuously for a charged and a discharged battery. The results are plotted in Fig. 5. The battery was charged up to 4.30 V at 274 K for the upper figure, and discharged down to 2.75 V for the lower. In both figures, the heat flow of second and third scanning are almost the same and only that of the first scanning is larger. This suggests that the diffusion of lithium ions affects the heat generation during the first scan; however, the concentration gradient of lithium ions is not present for the second and third. When the specific heat capacity of the battery is measured the heating treatment is required at first to avoid lithium diffusion effects.

As a result of the charged state in Fig. 5, the higher temperature isothermal baseline 343 K, is still higher than that at the lower temperature, 273 K, even in the second or the third scan. In addition, they are higher than those of the discharged state. This means that there are other factors of heat generation depending on temperature and on the state of the battery. One of them is thought to be self-discharge. As described above, the efficiency of charge and discharge is extremely good in mild situation such as at a constant temperature of 303 K; however, it decreases to 98% and below at 333 K. This suggests that the self-discharge increases at high temperature and it causes heat generation. The temperature dependence of this heat was also studied calorimetrically. The battery was left in the calorimeter and the temperature was controlled isothermally for several hours. The heat flow observed was higher than that of a blank measurement using an empty holder, and the difference was assumed to be the heat of self-discharge. The results are plotted in Fig. 6. This experiment was repeated for a charged battery up to 4.30 V at 303 K and a discharged one at 2.75 V. Before the measurement, the battery was heated to 343 K to eliminate the effect of lithium diffusion. In Fig. 6, the temperature is higher, the heat of self-discharge is larger in both states of the battery. This is one of the reasons why the isothermal baselines at 343 K in Fig. 2 are greater. The heat treatment is important in removing the nonuniform distribution of lithium ions; however, the temperature has not so high as to prevent unnecessary reactions.

As shown in Fig. 6, the heat of the self-discharge is much larger in the charged state than that in discharged state. The battery is less stable in the charged state. Consequently, the specific heat capacity of the highly charged lithium ion battery, as in state (a), cannot be evaluated precisely in high temperature region.

The specific heat capacity of the lithium ion battery plotted in Fig. 3 were evaluated without considering the effect of the heat of lithium diffusion. As the self-discharge, its influence is normalized at the state (h) and the error due to choice of isothermal baseline is atmost 1.5% in the states between (d) and (i). The heat of lithium diffusion is considered to be small between (c) and (i) because the isothermal baselines at 343 K were almost constant with little decay. Therefore, we can discuss the changes in the specific heat capacity of the battery during discharge except in the early and in last stages. Fig. 3 shows the decrease in the specific heat capacity with discharging as a result of the electrode materials which are varying in the battery reaction, and lithium ions move from the negative electrode to the positive during discharge. Interaction of the lithium ions with the host materials constructing lattice framework in the positive electrode is probably stronger than that in the negative electrode.

5. Conclusion

The twin-type heat conduction calorimeter was sufficiently reliable and accurate to study the

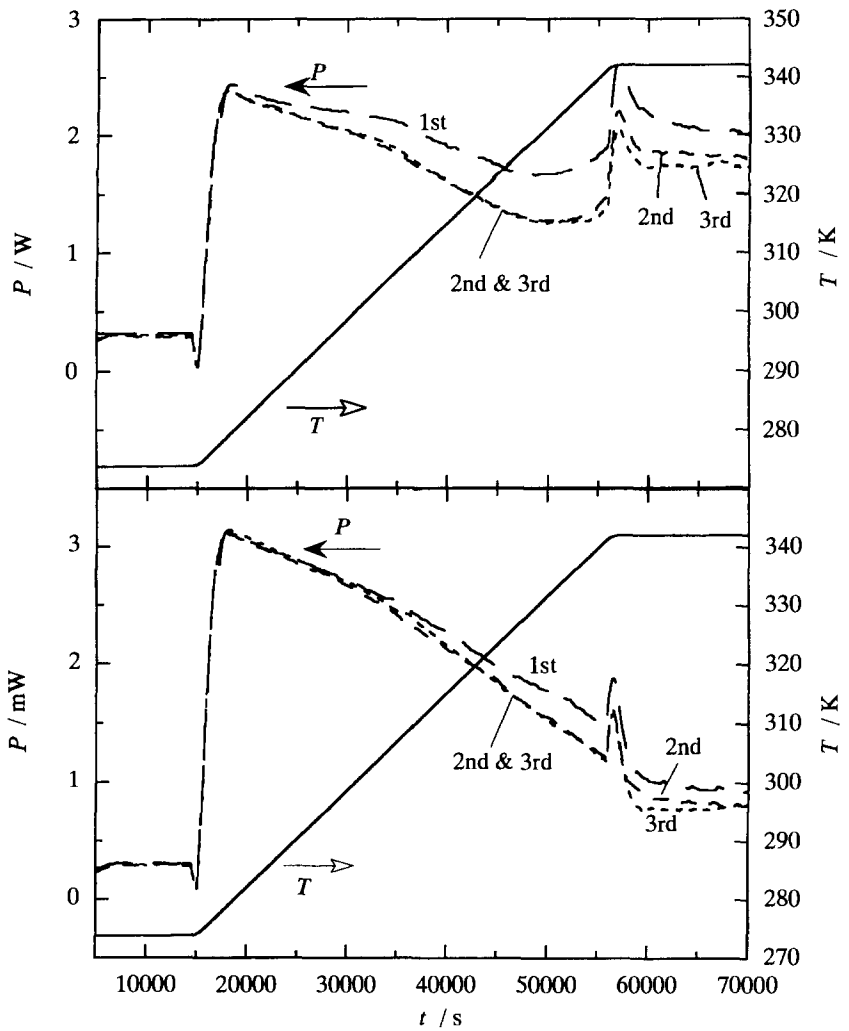

Fig. 5. Heat flow of a lithium ion battery during temperature scanning from 273 to 343 K. Charged state in upper figure and discharged state in lower. Scanning was carried out three times continuously.

thermal properties of the cylindrical type lithium ion battery whose size was 14 mm in diameter and 50 mm in length. The accuracy of the measurements were atmost 1.1% in the specific heat capacity measurements of synthetic sapphire. Apparent specific heat capacities of the battery were measured. A decrease in value with discharge meant that interaction between lithium ions and host materials was stronger in the positive electrode than negative electrode. The heat generation by the diffusion of lithium ions in the electrode materials and the self-discharge was observed. There were phase transitions of the positive electrode material, $Li_{1-x}CoO_2$, and the transition from monoclinic to hexagonal phase was endothermic. This behaviour was observed in calorimeter during electrochemical reaction and temperature scanning.

Acknowledgements

The authors would like to thank Mr. Kunio Ishi who had been a managing director of SONY Energytec Inc. for providing lithium ion cells.

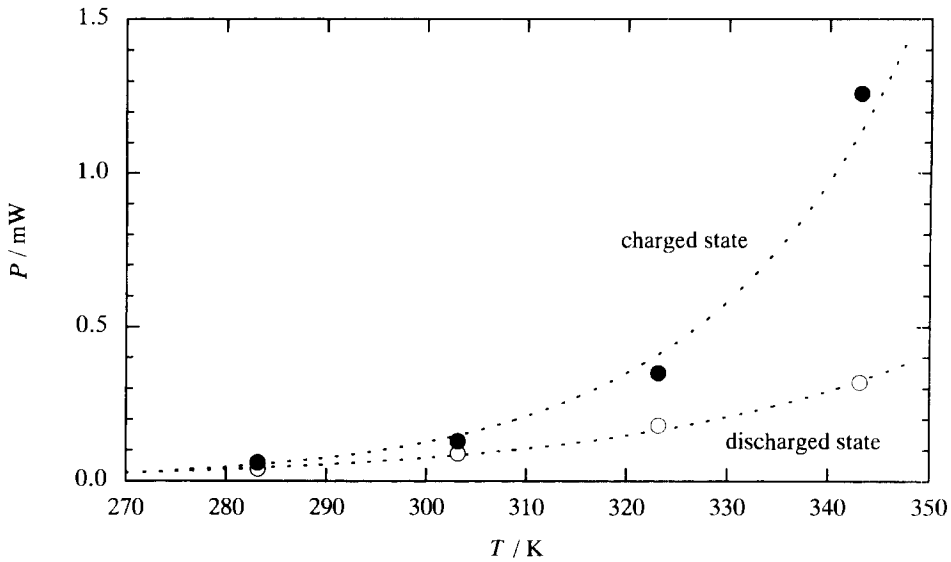

Fig. 6. Temperature dependence of the heat caused by self-discharge in a lithium ion battery. The states of the battery are (●) charged and (○) discharged.

References

[1] W.R. McKinnon, J.R. Dahn, J.J. Murray, R.R. Haering, P.C. McMillan and A.H. Rivers-Bowerman, J. Phys. C: Solid State Phys., 19 (1986) 5135.
[2] M. Nagamine, Kagakukogyo, 43 (1992) 945.
[3] M.C. Mraw, in: C.Y. Ho (Ed.), CINDAS Data Series on Material Properties, Vol. 1–2, Specific Heat of Solids, Hemisphere Publication Corporation, New York, 1988, p. 414.
[4] Y. Saito, K. Takano, K. Kanari and T. Masuda, manuscript in preparation.
[5] D.A. Ditmers and T.B. Douglas, J. Res. Natl. Stand, 75A (1971) 401.
[6] T. Ozuku, Y. Iwakoshi and K. Sawai, J. Electrochem. Soc., 140 (1993) 2490.
[7] J.N. Reimers and J.R. Dahn, J. Electrochem. Soc., 139 (1992) 2091.
[8] M.G.S.R. Thomas, P.G. Bruce and J.B. Goodenough, Solid State Ionics, 17 (1985) 13.
[9] T. Uchida, T. Itoh, Y. Morikawa, H. Ikutu and M. Wakihara, Denki Kagaku, 61 (1993) 1390.